Research Article

CrossMark
click for updates

The Effects of Thymoquinone on Viability, and Anti-apoptotic Factors (BCL-XL, BCL-2, MCL-1) in Prostate Cancer (PC3) Cells: An *In Vitro* and Computer-Simulated Environment Study

Javad Saffari-Chaleshtori[1] , **Ehsan Heidari-Sureshjani**[2], **Fahimeh Moradi**[3], **Esfandiar Heidarian**[4*]

[1]Student Research Committee, Shiraz University of Medical Sciences, Shiraz, Iran.
[2]Young Researchers and Elites Club, Islamic Azad University, Shahrekord Branch, Shahrekord, Iran.
[3]Cellular & Molecular, Research Center, Basic Health Sciences Institute, Shahrekord University of Medical Sciences, Shahrekord, Iran.
[4]Clinical Biochemistry Research Center, Basic Health Sciences Institute, Shahrekord University of Medical Sciences, Shahrekord, Iran.

Abstract

Purpose: Since active plant ingredients can induce apoptosis in many tumors, in this study we evaluate the apoptotic effects of thymoquinone (TQ) on PC3 cells. Also, we predicted the interaction of TQ with BCL-XL, BCL-2, and MCL-1anti-apoptotic factors by computer-simulated environment.

Methods: PC3 cells were treated with different concentrations of TQ (0- 80 µM) and IC_{50} was determined using 3-(4, 5-dimethylthiaztol-2-yl)-2, 5-diphenyltetrazolium bromide (MTT) assay. Apoptotic and cytotoxicity effects of TQ were analyzed using flowcytometry and comet assay, respectively. Changes in energy and the molecular interactions of TQ with BCL-XL, BCL-2 and MCL-1 anti-apoptotic factors were investigated using simulation.

Results: IC_{50} value was 40 µM. TQ led to the destruction of the genome of PC3 cells and inducing apoptosis. Molecular dynamics (MD) revealed that the root mean-square deviation (RMSD), root mean square fluctuation (RMSF), radius of gyration (Rg), and the number of hydrogen and hydrophobic bonds between TQ and residues of BCL-2, BCL-XL and MCL-1were significantly ($P<0.001$) changed. TQ makes a more stable and stronger connection with BCL-XL compared to BCL-2 and MCL-1 and inhibits BCL-XL non-competitively.

Conclusion: Our results demonstrated that TQ not only led to apoptosis, at least partly, due to reduction in the Coil, Turn, and Bend structure of BCL-XL but also caused a decrease in the Rg and RMSD value of BCL-XL, MCL-1, and BCL-2.

Introduction

Nowadays, cancer is one of the most important concerns worldwide and has persuaded many scientists to perform extensive studies to know more about the mechanism underlying its development and also the approaches to prevent and cure the disease.[1,2] Prostate cancer (PC) is the most prevalent cancer in men and is the second leading cause of death due to cancer after lung cancer in males.[3] PC is initially dependent on androgens for proliferation, but eventually progresses to be androgen-independent phenotype PC in the androgen-independent phenotype becomes highly resistant to chemotherapy in advanced stages of the disease.[4]Androgen ablation therapy is mainly used for the treatment of hormone-sensitive PC. However, in most men usually after 2 to 3 years, metastatic PC leads to an androgen-independent state.[5] Many of the natural plant ingredients play an important role in cancer

prevention.[6] These natural compounds such as alkaloids, terpenes, lignans and flavonoids in various plants have anti-tumor properties.[7] Thymoquinone (2-isopropyl-5-methyl-1,4-benzoquinone) (TQ) is a bioactive plant ingredient which is abundantly found in plants such as *Nigella sativa* Linn.[8] TQ has been reported to have antioxidant,[9] anti-inflammatory,[10] anti-neoplastic[11] and anti-poisoning activities in malignancies such as PC,[12] osteosarcoma,[13] fibro sarcoma[14] and myeloblastic leukemia.[15] This compound has a strong antioxidant effect by which it prevents tumor cell growth in many cancers.[16]

Inhibition of cancer cell growth is often achieved by the activation of apoptotic regulatory factors. BCL-2, MCL-1and BCL-XL have been identified as three important factors in this pathway.[17] BCL-2 family plays a key role in regulation and inhibition of apoptosis and increase in its activity gives rise to a wide spectrum of cancers.[18]

*Corresponding Author: Esfandiar Heidarian, Tel: 038-33331471, Fax: 038-33330709, Email: heidarian_e@skums.ac.ir

Reduction in BCL-2 gene expression is the hallmark of the beginning of apoptosis which reinforces the effects of anti-tumor therapy. Over expression of BCL-2 causes resistance to anti-cancer therapy. BCL-2 interacts with a subset of pre-apoptotic molecules including BAD, BAX, BIM, BAK, BID, and BIK directly.[19] Also, BCL-XL and MCL-1, as anti-apoptotic factors, play a critical role in the inhibition of apoptosis.[20] Therefore, the aim of this study was to determine the genotoxic effects of TQ on PC3 cell line as well as predicting interactional molecular dynamic (MD) mechanisms of TQ with BCL-XL, BCL-2, and MCL-1 anti-apoptotic factors by computer-simulated environment based on molecular docking software (Auto Dock, Gromacs and VMD).

Materials and Methods

The human PC cell line, PC3, was purchased from Pasteur Institute of Iran (Tehran, Iran). TQ was obtained from Santa Cruz Biotechnology Inc. (Santa Cruz, CA, USA). RPMI 1640 medium and fetus bovine serum (FBS) were prepared from Gibco (Rockville, MD, USA). Pen/Strep antibiotics were purchased from Abcam (San Francisco, CA, USA). 3-(4,5-dimethylthiaztol-2-yl)-2,5-diphenyltetrazolium bromide (MTT) was purchased from Sigma-Aldrich (St. Louis, MO). All other chemicals used were of analytical grade.

Experimental Methods
Cell culture
PC3 cell line was cultured in RPMI1640 medium supplemented with 10%heat-inactivated FBS, penicillin (100 U/mL) and streptomycin (100 U/mL). The flasks were kept in a humidified incubator containing 5% CO_2 at 37°C.[21]

Cell viability
The viability of cells against cytotoxic effects of TQ was performed by MTT colorimetric assay. Briefly, 5×10^3 cells were cultured in a 96-well plate containing RPMI 1640 phenol-red free medium, supplemented with 10% FBS. After overnight incubation, cells were treated with different concentrations of TQ (0- 80 µM) for 48 h in a humidified 5% CO2 incubator.[21] Then, cells were treated with 12mM MTT solution and were incubated for 4 h. Optical density was measured at 490 nm with 670 nm as the reference wavelength by a micro plate reader (Stat Fax-2100, Spain). Each test was carried out in triplicate. Viability percentage was calculated as follows: (OD value of treated group/OD value of control group) 100× and non-treated cell viability was set as 100%.[22]

Alkaline electrophoresis and comet assay
Based on IC_{50} value 20 and 30 µM of TQ concentrations, (two concentrations lower than IC_{50}) were used in alkaline electrophoresis. PC3 untreated cells were used as negative control and positive control was treated with 50µM

H_2O_2.[23] Slides were cleaned by methanol and heated gently. A 300 µL of 1% agarose dissolved in PBS was poured on slides and after inserting lamella, the slides were put on ice packs to harden the first agarose layer. Slides were incubated at 37°C for 24 h, after removing lamella. 10 µL of prepared cells was mixed with 80 µL of 1 % low melting point agarose in PBS. Then, 10 µL of the solution was poured over the first layer of agarose and the lamella was immediately inserted to make the middle layer. The third layer of agarose was made using 1% agarose in PBS. Slides were incubated for 24hin lysis buffer containing 100 mM Na_2 EDTA, 10% DMSO and 2.5 mM NaCl, pH 10, and 1% triton X-100. In the next step, slides exposed to alkaline buffer solution containing 1 mM Na_2EDTA, 0.3 M NaCl and pH=13 for 30 minutes. The slides were subjected to electrophoresis (25V, 300 mA, and 40 min). Then, slides were rinsed three times using neutralizing solution comprising 0.4M Tris HCl (pH 7.5). Slides were fixed in 95% ethanol three times, stained in 20 µg/mL ethidium bromide and finally analyzed using fluorescent microscope with 40X magnification (Olympuse BX51, Tokyo, Japan). One hundred cell images were analyzed for each concentration using CASP v.1.2.2 software.[24]

Flowcytometry
PC3 cells were cultured in 6-well plates at a density of 1×10^4/well and were treated with three different concentrations of TQ (20, 30, and 40 µM). After treating PC3 cells with TQ for 48h, cells were harvested and washed twice with PBS. Then, the PC3 cells were mixed with binding buffer and incubated with an annexin-V/PI double staining solution at room temperature for 15 minutes according to the manufacture's protocol. Then, the 12 000 stained cells were analyzed by flow cytometry and the percentage of apoptotic cells was calculated.

Simulation and Molecular Dynamics (MD) of proteins
Protein structure of anti-apoptotic proteins including BCL-2, BCL-XL, and MCL-1 were obtained from the RCSB protein data bank with PDB ID: 2W3L, 2YXJ, and 3KZ0, respectively. PubChem compound databank (from National Center for Biotechnology Information) was used to obtain the structure of TQ with CID: 10281. For docking simulations, by applying the automated docking tool (AutoDock), the hetero atoms were removed and H-atoms were added to the protein structures.[25] MD simulation of BCL-2, BCL-XL, and MCL-1 in absence of TQ was done by Gromacs software v. 4.5.4.

Molecular docking
Docking simulation studies were conducted on three anti-apoptotic proteins and TQ using Lamarckian genetic algorithm (LGA) method[26] with automated docking tool (AutoDock 4.2.3 version). For each protein, a virtual network with x,y,z dimensions was created, though the size of the box has been changed depending on the TQ

size. AutoDock grids were calculated for regularly spaced points at intervals of 0.375 A° contained within a cube based on the BCL-2, BCL-XL, and MCL-1. Other docking parameters were left at the software's default values set. LGA was selected to specify the best conformations in 200 independent trials of each TQ. Also, the LigPlot plus v.2.1 software was used to describe protein–ligand interactions between the TQ and amino acids.

MD simulation of protein-ligand complexes

MD simulation of BCL-2, BCL-XL, and MCL-1 docked with TQ was ran by Gromacs v.4.5.4 software as described previously.[27] The temperature was set to 300 K for all the simulation times. In this study, docking and dynamic simulations were performed using bit system with Intel® Core™ i7 CPU Server.

Statistical analysis

Flowcytometry analysis was performed with GraphPad Prism 5 software. All the data were analyzed using Statistical Package for the Social Sciences software, version 22 (SPSS, Inc., Chicago, IL, USA). Inhibitory concentration of 50% (IC_{50}) was calculated by the Probit procedure. The alkaline comet assay parameters were calculated by one-way ANOVA followed by Tukey post hoc test. Paired-sample t test was used for MD analysis. P value less than 0.001 was considered significant.

Results and Discussion

Today, extensive studies have been carried out to reduce the mortality and morbidity of cancer diseases. During recent years, plant drugs and their derived compounds have attracted the attention of many scientists.[28] Some studies have revealed that some of these compounds are able to induce or inhibit apoptosis in tumor cells.[29]

Our findings showed that TQ can induce apoptosis strongly in PC3 cells. Figure 1 shows the cytotoxicity effects of TQ on PC3 cells. TQ declined the cell viability percentage gradually with the elevation of TQ concentration after 48 h. In our study, the IC_{50} value of TQ was 40μM which is in line with previous study.[30] It is reported that TQ can induce a significant up-regulation of reactive oxygen species (ROS) expression and free radicals in PC3 cells which lead to catalyze oxidation of lipids and oxidize cysteine residues in proteins accompanied by
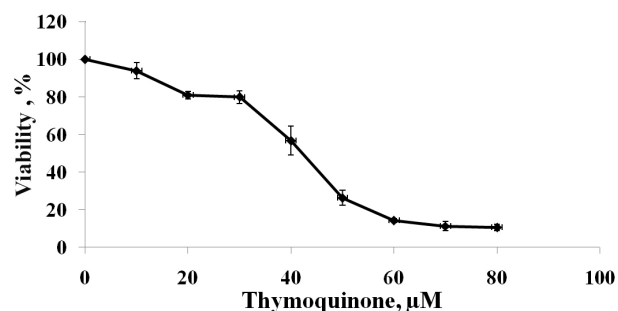

Figure 1. Inhibitory effects of TQ on PC3 cells viability. The viability of PC3 cells was measured by MTT assay for 48h at various concentrations of TQ. The data are expressed as mean ± SD three independent observations.

altering protein structure and function. These changes due to ROS may lead to growth inhibition.[31] Therefore, the reduction in PC3 cells viability in our study can result from, at least partly, ROS expression and free radicals.

In the present study, the effects of TQ at different concentrations on DNA fragmentation of PC3 cells were surveyed by comet assay (Table 1, Figure 2). The tail/head ratios of DNA were elevated by a dose dependent manner of TQ and maximized at IC_{50} concentration (40 μM) for negative control and treated cells. The ratio of the tail to head diameter on image D was higher, compared to other images. The tail/head cell ratio diameter is regarded as an appropriate criterion to determine the intensity of breakage. The ratios less than 10% displayed minor damage while higher ratios were considered as an indicator of severe or major damage. In our study, positive control (cells treated with 50 μM H_2O_2) had the longest tail which implied severe damage of the genome (Table 1). In the present study, the concentrations higher than IC_{50} led to cell death and determination of genome breakage was not assessed by comet assay. Also, our results show that the concentration of 40 μM has inflicted the most damage on PC3 cancer cells (Table 1).

DNA fragmentation is a hallmark of apoptosis that increasing *via* ROS production by TQ treated in PC3 cells.[32] Therefore, in the present study DNA-damage can take place by ROS production which induces apoptosis. Figure 3 represents the percentage of apoptosis and necrosis after treating the cells at different concentrations of TQ (0, 20, 30, and 40 μM) related to control cells.

Table 1. Genotoxicity Effects of TQ on PC3 Cells

Parameter	n	Control (A)	20 μM (B)	30 μM (C)	40 μM (D)	H_2O_2 50 μM (E)
Head DNA	100	43.3±0.7	8.2±0.2[a]	3.4±0.3[ab]	4.6±0.5[ab]	6.6±0.5[ac]
Tail DNA	100	0.8±0.1	2.0±0.1[a]	4.3±0.1[ab]	10.2±1.3[abc]	15.0±1.1[abc]
Head DNA%	100	98.2±0.1	79.7±0.7[a]	40.4±1.0[ab]	33.5±0.3[abc]	32.8±0.5[abc]
Tail DNA%	100	1.8±0.1	20.3±0.7[a]	59.6±1.0[ab]	66.5±0.3[abc]	67.2±0.5[abc]

A, B, C, and D are treated groups with 0 (negative control), 20, 30, and 40 μM of TQ respectively. E is positive control, a treated group with 50 μM H_2O_2. Head DNA; amount of DNA in the comet head, Tail DNA; amount of DNA in the comet tail, Head DNA%; percentage of DNA in the comet head to comet tail, and Tail DNA%; percentage of DNA in the comet tail to comet head. Statistical analysis was calculated by One-way ANOVA test. Each point represents mean ± SD.
[a]$P<0.001$ compared with group A; [b]$P<0.001$ compared with group B; [c]$P<0.001$ compared with group C.
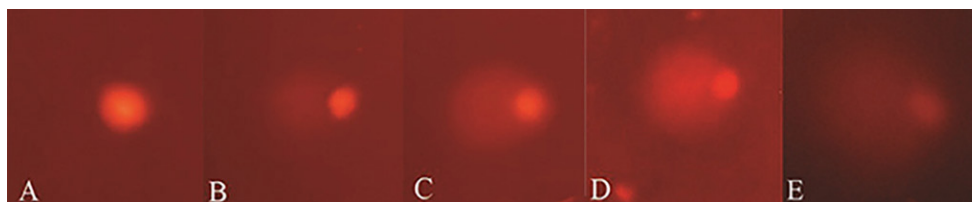
Figure 2. Genotoxicity effects of TQ on PC3 cells. (A) Negative control cells (without any tail), (B-D) cells treated with 20, 30, 40 µM concentrations of TQ respectively, € Cells treated with H_2O_2.
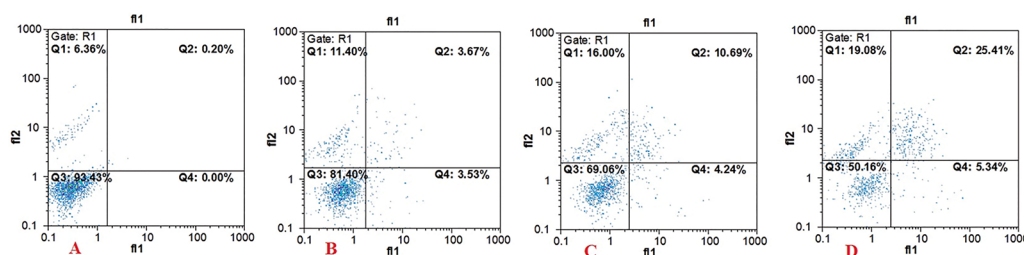

Figure 3. Apoptotic effects of TQ on PC3 cells after 48 h compared with control group using flowcytometry procedure. A; Negative control cells, B-D; cells treated with 20, 30 and 40 µM of TQ respectively.

Our results showed that the percentage of apoptosis was elevated more than that of necrosis which is in line with the previous study in GlioblastomaT-98G cells line.[33]

Also, Zhang et al showed that TQ can induce apoptosis *via* endoplasmic reticulum stress-dependent mitochondrial pathway, mitochondrial dysfunction, and activating the mitochondrion-mediated apoptotic pathway through reducing MCL-1 and MCL-XL, elevating BAX, AIF, and releasing cytochrome c.[34] It is reported that using MD simulation studies with *Panax ginseng* derived compounds can strongly attach to three anti-apoptotic proteins including MCL-XL, MCL-1, and BCL-2 and inhibit their activities.[35] In this study, MD simulation and docking results showed that TQ can strongly affect the MD of MCL-XL, MCL-1, and BCL-2.

Table 2 shows the binding energy (BE), final intermolecular energy (FIE), and estimated inhibition constant (EIC) of BCL-2, BCL-xl and MCL-1. According to our docking results, the lowest value of ΔG (BE) was between BCL-XL protein and TQ (Table 2). Therefore, the binding affinity of TQ to BCL-XL is higher than BCL-2 and MCL-1.

The LigPlot plus results (Figure 4) showed that TQ forms eight, six, and eight hydrophobic bonds on residues of BCL-2, MCL-1, and BCL-XL, respectively. However, no

hydrogen bond was found between TQ and them.

Figure 5 shows the active sites of BCL-2, BCL-XL and MCL-1 molecules with lowest energy which are connected to TQ.

A common criterion to assess the molecular dynamic simulation and also to validate its accuracy is determining the root mean-square deviation (RMSD) value of the protein backbone compared to the initial structure during simulation. This parameter is considered as an indicator of the simulation quality and also attainment or non-attainment of the equilibrium state in the simulation system. When a simulation is running, the more RMSD for one atom or a group of atoms indicate that their structures have more variations.[36]

According to Table 3, MCL-1 molecule shows the highest variation in RMSD which has been increased in the presence of TQ. In the presence of TQ, RMSD of BCL-XL protein was reduced, subsequently, the structure changes decreased and the molecule became more stable. Therefore, it can be concluded that TQ has the more powerful inhibition effect on BCL-XL than BCL-2 and MCL-1.

To assess the oscillation of each residue, we measured root mean square fluctuation (RMSF) to observe the flexibility of key residues. RMSF values in the presence of

Table 2. Molecular interaction between TQ and BCL-2, BCL-XL, and MCL-1

Receptor	BE kcal/mol	FIE kcal/mol	EIC µM	Interaction bonds	
				Hydrogen Bonding	Hydrophobic Bonding
BCL-2	-4.65	-5.55	388.7	-	Tyr139, Arg142, His143, Glu138, Ala90, Arg86, Phe89, Trp135
BCL-XL	-5.89	-6.79	47.94	-	Pro116, Gly117, Ala119, Trp169, Arg165, Tyr120
MCL-1	-4.64	-5.53	397.2	-	Glu16, Asn223, Asn17, Gly219, Tyr21, Arg215, Val216, Tyr20

Abbreviations: BE, binding and Energy (kcal/mol); FIE, final intermolecular energy (kcal/mol); EIC, estimated inhibition constant (µM).
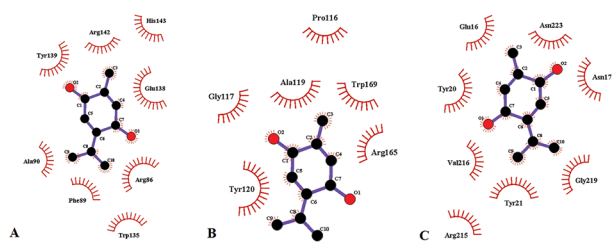
Figure 4. Analyzed protein–ligand interactions BCL-2 (A), BCL-XL (B), and MCL-1 (C).
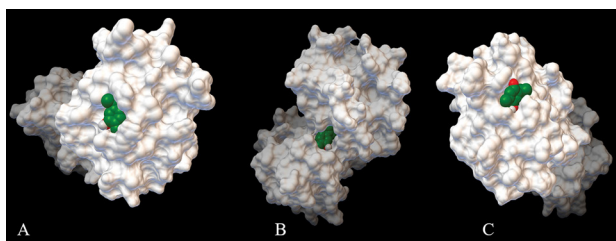

Figure 5. Three-dimensional structure of docked molecules between TQ and BCL-2 (A), BCL-XL (B), and MCL-1 (C).

Table 3. Molecular dynamic parameters

Protein		Rg	RMSD	RMSF
Bcl-2	G_1	2.22±0.020	0.58±0.112	0.190±0.061
	G_2	2.21±0.033[a]	0.25±0.057[a]	0.250±0.080[a]
Bcl-xl	G_1	1.96±0.016	0.68±0.043	0.205±0.072
	G_2	1.40±0.005[a]	0.32±0.010[a]	0.155±0.080[a]
Mcl-1	G_1	2.89±0.023	0.27±0.04	0.160±0.056
	G_2	2.48±0.027[a]	0.68±0.15[a]	0.330±0.120[a]

Abbreviations: G_1, simulation before docking; G_2, simulation after docking; Rg, Radius of gyration; RMSF, root mean square fluctuation; RMSD, root mean-square deviation.
Statistical analysis was calculated by paired-sample t test. Each point represents mean ± SD.
[a] $P < 0.001$ compared with group G_1.

TQ for the BCL-2 and MCL-1 increased but for BCL-XL decreased (Table 3).

Radius of gyration (Rg) is a scale of the protein radius. For globular proteins, the more Rg means the less compaction of the protein structure and more function. In the presence of an effective drug, Rg of the protein changes and subsequently its structure is altered.[37] This study showed that, TQ could decrease the Rg properties of these anti-apoptotic factors significantly. But, the most effect of TQ was on BCL-XL and MCL-1 (Figure 6 and Table 3).

The variations in the secondary structures of MCL-1, BCL-XL, and BCL-2 and the values of these variations as a single molecule or in complex with TQ are displayed in Table 4. According to the variation in the secondary structure parameter of the studied proteins, it seems that when TQ binds to BCL-XL, alpha-helix structure of the protein decreases and Bend, Turn and Coil structures
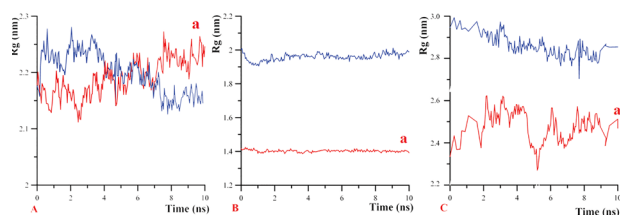

Figure 6. Radius of gyration (Rg) for BCL-2 (A), BCL-XL (B) and MCL-1 (C). Blue color; simulated anti-apoptotic factors in the absence of TQ and red color; simulated anti-apoptotic factors in the presence of TQ. Statistical analysis was calculated by Paired-sample t test. Each point represents mean±SD. [a] $P < 0.001$ compared with Blue color.

Table 4. The variations in secondary structure of MCL-1, BCL-XL and BCL

Protein		Coil	Bend	Turn	α-Helix
Bcl-2	G_1	41.87±2.09	14.10±3.20	22.45±4.06	201.86±3.88
	G_2	42.13±2.18[a]	16.95±2.94[a]	21.31±4.02[a]	201.70±3.87
Bcl-xl	G_1	38.96±1.7	13.21±3.20	24.87±4.80	199.56±6.03
	G_2	19.45±1.7[a]	7.45±2.41[a]	11.62±3.65[a]	194.92±4.16[a]
Mcl-1	G_1	47.36±2.07	18.42±2.90	22.58±3.75	244.76±3.17
	G_2	47.47±2.45	22.22±4.45[a]	23.75±4.76[a]	239.90±4.18[a]

Abbreviations: G_1, simulation before docking; G_2, simulation after docking.
Statistical analysis was calculated by paired-sample t test. Each point represents mean±SD.
[a] $P < 0.001$ compared with group G_1.

decrease significantly (Table 4). Since alpha helix and beta-sheet structures exist in structural regions of proteins and turn and coil structures mostly exist in functional regions.[38] It is hypothesized that in this state, BCL-XL is less effective. MCL-1 and BCL-2 molecule displayed fewer variations than BCL-XL. However, some of these variations are significant but the biggest 2D structure variation is related to BCL-XL.

Conclusion

This study showed that TQ at the concentrations close to IC_{50} can damage PC3 PC cells and also induce apoptosis more than necrosis. Molecular docking results and analysis revealed that TQ makes more stable bonds with BCL-XL than BCL-2 and MCL-1. RMSD data indicated that TQ inhibits BCL-XL non-competitively, so by inhibiting BCL-XL and less MCL-1, TQ can induce apoptosis. MD results indicated that TQ has the lowest influence on MCL-1. The changes in the secondary structure showed that TQ exerts drastic changes over BCL-Xl molecule by reducing the effective 2D structures. Taken together, our study revealed that TQ induces apoptotic effects by inhibiting the anti-apoptotic factor BCL-XL protein compared to other studied factors.

Ethical Issues

The current article does not contain any studies with human or animal subjects.

Conflict of Interest

Acknowledgments

References

1. Valerio M, Donaldson I, Emberton M, Ehdaie B, Hadaschik BA, Marks LS, et al. Detection of clinically significant prostate cancer using magnetic resonance imaging-ultrasound fusion targeted biopsy: a systematic review. *Eur Urol* 2015;68(1):8-19. doi: 10.1016/j.eururo.2014.10.026

2. Saffari-Chaleshtori J, Tabatabaiefar MA, Ghasemi-Dehkordi P, Farokhi E, Moradi MT, Hashemzadeh-Chaleshtori M. The lack of correlation between TP53 mutations and gastric cancer: a report from a province of Iran. *Genetika* 2017;49(1):235-46. doi: 10.2298/gensr1701235S

3. Ferlay J, Colombet M, Soerjomataram I, Mathers C, Parkin DM, Pineros M, et al. Estimating the global cancer incidence and mortality in 2018: GLOBOCAN sources and methods. *Int J Cancer* 2019;144(8):1941-53. doi: 10.1002/ijc.31937

4. Vlachostergios PJ, Papandreou CN. Targeting neuroendocrine prostate cancer: molecular and clinical perspectives. *Front Oncol* 2015;5:6. doi: 10.3389/fonc.2015.00006

5. de Leeuw R, Berman-Booty LD, Schiewer MJ, Ciment SJ, Den RB, Dicker AP, et al. Novel actions of next-generation taxanes benefit advanced stages of prostate cancer. *Clin Cancer Res* 2015;21(4):795-807. doi: 10.1158/1078-0432.ccr-14-1358

6. Harris IS, Treloar AE, Inoue S, Sasaki M, Gorrini C, Lee KC, et al. Glutathione and thioredoxin antioxidant pathways synergize to drive cancer initiation and progression. *Cancer Cell* 2015;27(2):211-22. doi: 10.1016/j.ccell.2014.11.019

7. Uruena C, Cifuentes C, Castaneda D, Arango A, Kaur P, Asea A, et al. Petiveria alliacea extracts uses multiple mechanisms to inhibit growth of human and mouse tumoral cells. *BMC Complement Altern Med* 2008;8:60. doi: 10.1186/1472-6882-8-60

8. Gali-Muhtasib HU, Abou Kheir WG, Kheir LA, Darwiche N, Crooks PA. Molecular pathway for thymoquinone-induced cell-cycle arrest and apoptosis in neoplastic keratinocytes. *Anticancer Drugs* 2004;15(4):389-99.

9. Badary OA, Taha RA, Gamal el-Din AM, Abdel-Wahab MH. Thymoquinone is a potent superoxide anion scavenger. *Drug Chem Toxicol* 2003;26(2):87-98. doi: 10.1081/dct-120020404

10. El Gazzar M, El Mezayen R, Marecki JC, Nicolls MR, Canastar A, Dreskin SC. Anti-inflammatory effect of thymoquinone in a mouse model of allergic lung inflammation. *Int Immunopharmacol* 2006;6(7):1135-42. doi: 10.1016/j.intimp.2006.02.004

11. Gali-Muhtasib H, Ocker M, Kuester D, Krueger S, El-Hajj Z, Diestel A, et al. Thymoquinone reduces mouse colon tumor cell invasion and inhibits tumor growth in murine colon cancer models. *J Cell Mol Med* 2008;12(1):330-42.

doi: 10.1111/j.1582-4934.2007.00095.x

12. Kaseb AO, Chinnakannu K, Chen D, Sivanandam A, Tejwani S, Menon M, et al. Androgen receptor and E2F-1 targeted thymoquinone therapy for hormone-refractory prostate cancer. *Cancer Res* 2007;67(16):7782-8. doi: 10.1158/0008-5472.can-07-1483

13. Roepke M, Diestel A, Bajbouj K, Walluscheck D, Schonfeld P, Roessner A, et al. Lack of p53 augments thymoquinone-induced apoptosis and caspase activation in human osteosarcoma cells. *Cancer Biol Ther* 2007;6(2):160-9. doi: 10.4161/cbt.6.2.3575

14. Ivankovic S, Stojkovic R, Jukic M, Milos M, Milos M, Jurin M. The antitumor activity of thymoquinone and thymohydroquinone in vitro and in vivo. *Exp Oncol* 2006;28(3):220-4.

15. El-Mahdy MA, Zhu Q, Wang QE, Wani G, Wani AA. Thymoquinone induces apoptosis through activation of caspase-8 and mitochondrial events in p53-null myeloblastic leukemia HL-60 cells. *Int J Cancer* 2005;117(3):409-17. doi: 10.1002/ijc.21205

16. Banerjee S, Padhye S, Azmi A, Wang Z, Philip PA, Kucuk O, et al. Review on molecular and therapeutic potential of thymoquinone in cancer. *Nutr Cancer* 2010;62(7):938-46. doi: 10.1080/01635581.2010.509832

17. Ouyang L, Shi Z, Zhao S, Wang FT, Zhou TT, Liu B, et al. Programmed cell death pathways in cancer: a review of apoptosis, autophagy and programmed necrosis. *Cell Prolif* 2012;45(6):487-98. doi: 10.1111/j.1365-2184.2012.00845.x

18. Llambi F, Green DR. Apoptosis and oncogenesis: give and take in the BCL-2 family. *Curr Opin Genet Dev* 2011;21(1):12-20. doi: 10.1016/j.gde.2010.12.001

19. Engel T, Henshall DC. Apoptosis, Bcl-2 family proteins and caspases: the ABCs of seizure-damage and epileptogenesis? *Int J Physiol Pathophysiol Pharmacol* 2009;1(2):97-115.

20. Volkmann N, Marassi FM, Newmeyer DD, Hanein D. The rheostat in the membrane: BCL-2 family proteins and apoptosis. *Cell Death Differ* 2014;21(2):206-15. doi: 10.1038/cdd.2013.153

21. Kaur M, Velmurugan B, Rajamanickam S, Agarwal R, Agarwal C. Gallic acid, an active constituent of grape seed extract, exhibits anti-proliferative, pro-apoptotic and anti-tumorigenic effects against prostate carcinoma xenograft growth in nude mice. *Pharm Res* 2009;26(9):2133-40. doi: 10.1007/s11095-009-9926-y

22. Kumi-Diaka J, Sanderson NA, Hall A. The mediating role of caspase-3 protease in the intracellular mechanism of genistein-induced apoptosis in human prostatic carcinoma cell lines, DU145 and LNCaP. *Biol Cell* 2000;92(8-9):595-604. doi: 10.1016/S0248-4900(00)01109-6

23. Benhusein GM, Mutch E, Aburawi S, Williams FM. Genotoxic effect induced by hydrogen peroxide in human hepatoma cells using comet assay. *Libyan J Med* 2010;5. doi: 10.3402/ljm.v5i0.4637

24. Allahbakhshian-Farsani M, Abdian N, Ghasemi-Dehkordi P, Sadeghiani M, Saffari-Chaleshtori J, Hashemzadeh-Chaleshtori M, et al. Cytogentic analysis of human dermal fibroblasts (HDFs) in early and late passages using both karyotyping and comet assay techniques. *Cytotechnology* 2014;66(5):815-22. doi: 10.1007/s10616-013-9630-y

25. Rarey M, Kramer B, Lengauer T, Klebe G. A fast flexible docking method using an incremental construction

algorithm. *J Mol Biol* 1996;261(3):470-89. doi: 10.1006/jmbi.1996.0477

26. Morris GM, Goodsell DS, Halliday RS, Huey R, Hart WE, Belew RK, et al. Automated docking using a Lamarckian genetic algorithm and an empirical binding free energy function. *J Comput Chem* 1998;19(14):1639-62. doi: 10.1002/(sici)1096-987x(19981115)19:14<1639::aid-jcc10>3.0.co;2-b

27. Saffari-Chaleshtori J, Heidari-Sureshjani E, Moradi F, Molavian Jazi H, Heidarian E. The study of apoptosis-inducing effects of three pre-apoptotic factors by gallic acid, using simulation analysis and the comet assay technique on the prostatic cancer cell line PC3. *Malays J Med Sci* 2017;24(4):18-29. doi: 10.21315/mjms2017.24.4.3

28. Heidarian E, Keloushadi M, Ghatreh-Samani K, Valipour P. The reduction of IL-6 gene expression, pAKT, pERK1/2, pSTAT3 signaling pathways and invasion activity by gallic acid in prostate cancer PC3 cells. *Biomed Pharmacother* 2016;84:264-9. doi: 10.1016/j.biopha.2016.09.046

29. Elmore S. Apoptosis: a review of programmed cell death. *Toxicol Pathol* 2007;35(4):495-516. doi: 10.1080/01926230701320337

30. Koka PS, Mondal D, Schultz M, Abdel-Mageed AB, Agrawal KC. Studies on molecular mechanisms of growth inhibitory effects of thymoquinone against prostate cancer cells: role of reactive oxygen species. *Exp Biol Med (Maywood)* 2010;235(6):751-60. doi: 10.1258/ebm.2010.009369

31. Higuchi Y. Glutathione depletion-induced chromosomal DNA fragmentation associated with apoptosis and necrosis. *J Cell Mol Med* 2004;8(4):455-64. doi: 10.1111/j.1582-4934.2004.tb00470.x

32. Zeng CC, Lai SH, Yao JH, Zhang C, Yin H, Li W, et al. The induction of apoptosis in HepG-2 cells by ruthenium(II) complexes through an intrinsic ROS-mediated mitochondrial dysfunction pathway. *Eur J Med Chem* 2016;122:118-26. doi: 10.1016/j.ejmech.2016.06.020

33. Kus G, Ozkurt M, Kabadere S, Erkasap N, Goger G, Demirci F. Antiproliferative and antiapoptotic effect of thymoquinone on cancer cells in vitro. *Bratisl Lek Listy* 2018;119(5):312-6. doi: 10.4149/bll_2018_059

34. Zhang M, Du H, Huang Z, Zhang P, Yue Y, Wang W, et al. Thymoquinone induces apoptosis in bladder cancer cell via endoplasmic reticulum stress-dependent mitochondrial pathway. *Chem Biol Interact* 2018;292:65-75. doi: 10.1016/j.cbi.2018.06.013

35. Sathishkumar N, Sathiyamoorthy S, Ramya M, Yang DU, Lee HN, Yang DC. Molecular docking studies of anti-apoptotic BCL-2, BCL-XL, and MCL-1 proteins with ginsenosides from Panax ginseng. *J Enzyme Inhib Med Chem* 2012;27(5):685-92. doi: 10.3109/14756366.2011.608663

36. Carugo O, Pongor S. A normalized root-mean-square distance for comparing protein three-dimensional structures. *Protein Sci* 2001;10(7):1470-3. doi: 10.1110/ps.690101

37. Lobanov MY, Bogatyreva NS, Galzitskaya OV. Radius of gyration as an indicator of protein structure compactness. *Mol Biol* 2008;42(4):623-8. doi: 10.1134/s0026893308040195

38. Cuff JA, Barton GJ. Evaluation and improvement of multiple sequence methods for protein secondary structure prediction. *Proteins* 1999;34(4):508-19. doi: 10.1002/(sici)1097-0134(19990301)34:4<508::aid-prot10>3.0.co;2-4